ENERGY LANDSCAPES AT FINITE ANGULAR MOMENTUM WITHIN THE FOURIER SHAPE PARAMETRIZATION* **

J. Bartel

IPHC, Université de Strasbourg, CNRS, 67037 Strasbourg, France

K. Pomorski, B. Nerlo-Pomorska

Department of Theoretical Physics, Maria Curie Skłodowska University
Radziszewskiego 10, 20-031 Lublin, Poland

(Received January 17, 2017)

Deformation-energy landscapes for nuclei at finite angular momentum are presented and analysed with respect to possible shape transitions known as Maclaurin, Jacobi and Poincaré instabilities. To be able to perform such a study, it turns out that a vast variety of nuclear shapes needs to be considered. For such an analysis, we rely on the recently developed Fourier shape parametrization, together with the macroscopic–microscopic model, an approach which proves to yield excellent results.

DOI:10.5506/APhysPolBSupp.10.17

1. Introduction

One of the greatest challenges in the theory of nuclear structure and reactions consists in describing the enormous variety of shapes a nucleus can take, between the oblate side encountered in the transition region corresponding to the progressive filling of the pf shell and the prolate deformations realized in the rare-earth region, but much more so in the very large deformations found in the fission process. In some areas of the nuclear chart, on the contrary, the nuclear shape is very sensitive to structural effects and can change from one nucleus to its neighbour. Apart from these

* Presented at the XXIII Nuclear Physics Workshop "Marie and Pierre Curie", Kazimierz Dolny, Poland, September 27–October 2, 2016.

** This work has been partly supported by the Polish–French COPIN-IN2P3 collaboration agreement under project number 08-131 and by the Polish National Science Centre (NCN), grant No. 2013/11/B/ST2/04087.

very rapid shape changes with proton or neutron number, the shape can also change, within the same nucleus, with increasing excitation energy or angular momentum. Such changes are caused by a rearrangement of the orbital configuration of the nucleons or by a dynamic response of the nuclear system to rotation. It is this last effect that is the subject of the present investigation.

In a seminal publication, more than 40 years ago, Cohen, Plasil and Swiatecki [1] have investigated the equilibrium configurations of rotating charged or gravitating bodies (with a special emphasis on rotating nuclei), thus persuing the investigations of many illustrious mathematicians and physicists, such as Newton, Maclaurin, Jacobi, Riemann, Poincaré and Chandrasekhar on celestial bodies bound by the gravitational force. Let us, in particular, mention in this context the monumental work on *Ellipsoidal Figures of Equilibrium* [2] by Chandrasekhar. Exactly like in Lagrangian or Hamilton Mechanics, the equilibrium configurations are identified by a careful mapping of the potential energy as a function of the degrees of freedom. In the following, we will concentrate, as also done in Ref. [1], on the nuclear problem and consider only the macroscopic liquid-drop type contribution to the energy, thus describing the evolution with increasing angular momentum of the dominant nuclear bulk behaviour.

Apart from the smooth dependence of the nuclear shape on angular momentum, as this is observed at low values of the angular momentum, where the nucleus has the tendency to take on an oblate shape, known as the Maclaurin regime, there are two kinds of instabilities discussed in the literature already in the 19^{th} century: the Jacobi transition [2, 3] that preserves left–right symmetry but breaks axial symmetry at some critical value of the angular momentum, thus favouring triaxial shapes and the Poincaré instability [4] that breaks left–right symmetry, thus leading to pear-like deformations. After presenting the theoretical model used to investigate these shape transitions in Section 2, we will present in Section 3 some deformation energy landscapes for nuclei from different regions of the periodic table in order to identify the presence and locations of these transitions, where they exist. Conclusions and future fields of investigations are presented in Section 4.

2. Model

The nuclear deformation-energy landscapes that are presented below are determined in a liquid-drop type approach, where the macroscopic energy is evaluated in the Lublin–Strasbourg Drop (LSD) [5], that contains, in addition to the standard volume, surface and Coulomb contributions, a curvature (proportional to $A^{1/3}$) and a so-called *congruence energy* term [6]. All theses contributions, except for the volume term, carry their deformation depen-

dence. Thus approach has proven [5] not only to yield excellent nuclear masses, with an r.m.s. deviation from the experimental values of less than 0.7 MeV, but also to reproduce very well nuclear fission-barrier heights. Based on this macroscopic model, microscopic energy corrections can be taken into account through the Strutinsky shell corrections and pairing correlations, as determined *e.g.* through the BCS approach. In this way, one is able to obtain some quite precise evaluation of the nuclear deformation-energy landscape to a point where one is even able to make predictions about the fission-fragment mass distribution [7,8].

To go beyond this standard procedure and to be able to describe the nuclear structure at finite angular momentum, it is sufficient to add a rotational term to the LSD liquid-drop type energy, which then writes

$$\begin{aligned} E_{\rm mac}(Z,N;{\rm def}) \;=\; & a_{\rm v}\,\left(1-\kappa_{\rm vol}I^2\right)\,A + a_{\rm s}\,\left(1-\kappa_{\rm s}I^2\right)\,A^{2/3}\,B_{\rm s}({\rm def}) \\ & + a_{\rm c}\,\left(1-\kappa_{\rm c}I^2\right)\,A^{1/3}\,B_{\rm c}({\rm def}) + c_1\,\frac{Z^2}{A^{1/3}}\,B_{\rm Coul}({\rm def}) \\ & + c_2\,\frac{Z^2}{A} + E_{\rm cong}({\rm def}) + \frac{\hbar^2}{2\mathcal{J}_{\rm rig}}L(L+1)\,B_{\rm rot}({\rm def})\,. \quad (2.1) \end{aligned}$$

All the deformation dependence of $E_{\rm mac}$ is contained in the shape functions $B_{\rm k}$ (see *e.g.* [11]) and the congruence energy $E_{\rm cong}$ [6]. Since we are only concerned with the macroscopic nuclear energy in the present investigation, no pairing is present here, and the description of the rotational energy with a rigid-body moment of inertia is consistent.

As already pointed out in the introduction, it is absolutely essential for a correct description of the nuclear potential energy surface to be able to describe the physically relevant deformation degrees of freedom in a way, as close to the physical reality, as ever possible. In the past, we have worked for many years with the so-called *Modified Funny-Hills* parametrization [12] that has proven extremely successful, but which has the slight disadvantage that one is not able to test its convergence. We have recently proposed a Fourier expansion of the nuclear surface [13] that writes in cylindrical coordinates as

$$\frac{\rho_{\rm s}^2(z)}{R_0^2} = \sum_{n=1}^{\infty}\left[a_{2n}\cos\left(\frac{(2n-1)\pi}{2}\,\frac{z-z_{\rm sh}}{z_0}\right) + a_{2n+1}\sin\left(n\pi\,\frac{z-z_{\rm sh}}{z_0}\right)\right]\,, \quad (2.2)$$

where $\rho_{\rm s}(z)$ is the distance from the symmetry axis to the surface of the nucleus at coordinate z, and R_0 is the radius of the corresponding spherical shape having the same volume. The extension of the nuclear shape along the symmetry axis is $2z_0$ with left and right ends located at $z_{\rm min} = z_{\rm sh} - z_0$ and $z_{\rm max} = z_{\rm sh} + z_0$, where $\rho_{\rm s}^2(z)$ vanishes, a condition which is automatically

satisfied by Eq. (2.2). The shift coordinate $z_{\rm sh}$ is chosen such that the center of mass of the shape is always located at the origin of the coordinate system (see Refs. [8, 13] for a more detailed discussion).

It turns out [13] that the LD path to fission goes towards decreasing values of a_2 and growing negative values of a_4, which is somehow contrary to common practice. It is, therefore, convenient to introduce new, physically more intuitive, collective coordinates which ensure, in addition, an optimal presentation of the potential energy landscape and a fast convergence of the shape parametrization:

$$\begin{aligned} q_2 &= a_2^{(0)}/a_2 - a_2/a_2^{(0)}\,, \qquad q_3 = a_3\,, \quad q_4 = a_4 + \sqrt{(q_2/9)^2 + \left(a_4^{(0)}\right)^2} \\ q_5 &= a_5 - a_3(q_2-2)/10\,, \quad q_6 = a_6 - \sqrt{(q_2/100)^2 + \left(a_6^{(0)}\right)^2}\,, \end{aligned} \tag{2.3}$$

where $a_2^{(0)} = 1.03205$, $a_4^{(0)} = -0.03822$, and $a_6^{(0)} = 0.00826$ are the expansion coefficients for a sphere. These definitions (2.3) have been made in such a way that the bottom of the LD fission valley corresponds roughly to $q_4 = q_6 = 0$, and the definitions of q_5 and q_6 ensure the smallest stiffness of the LD energy towards q_3 and q_4, respectively, when $q_5 = q_6 = 0$. This means, as we will show in what follows below, that even for a collective motion as the fission process, where a very large variety of nuclear deformations is explored, all the encountered shapes can be described very precisely by only 4 deformation parameters.

Till now, we have only considered axially symmetric shapes. To be able to describe non-axial shapes, we assume that the cross section perpendicular to the z-axis has the form of an ellipse with half axis $a(z)$ and $b(z)$

$$\frac{x^2}{a^2} + \frac{y^2}{b^2} = 1\,. \tag{2.4}$$

In polar coordinates, the above equation leads then to the shape function

$$\varrho_{\rm s}^2(z,\varphi) = \rho_{\rm s}^2(z)\,\frac{1-\eta^2}{1+\eta^2+2\eta\cos(2\varphi)}\,, \tag{2.5}$$

where, to better distinguish the function $\varrho_{\rm s}(z,\varphi)$ from the surface parametrization in the axially symmetric case, as given by Eq. (2.2), we have thus introduced the two writings, $\rho_s(z)$ and $\varrho_{\rm s}(z,\varphi)$.

We are going to show in the following that with only 4 deformation parameters, namely a *quadrupole* parameter q_2, an *octupole* parameter q_3 and a *hexadecapole* parameter q_4, plus one non-axiality parameter η we are able to cover quite precisely all nuclear shapes encountered in the fission process and able to describe the shape transitions we are interested in.

3. Results

One of the possible transitions, we are particularly interested in, is the Poincaré instability that would favour asymmetric (pear-like) deformations relative to left–right symmetric ones. In the language of nuclear deformation energies, that would say that, in rotating nuclei, an asymmetric local minimum would be lower in energy than the corresponding symmetric one. In their pioneering publication [1], Cohen, Plasil and Swiatecki have predicted that such an instability should occur in a non-rotating nucleus for a fissility parameter $x \leq 0.4$ (the so-called Businaro–Gallone point) and that this tendency is even favoured with increasing rotational angular momentum. This analysis had been performed at that time with a rather crude macroscopic model and a very limited shape parametrization. One of the aims of the present investigation is to test these conclusions with a much more precise nuclear model as presented above. We first show in Fig. 1 the deformation-energy landscapes of four nuclei from different regions of the periodic table (and different fissility parameters x), namely $^{46}_{22}$Ti ($x \approx 0.21$), $^{90}_{40}$Zr ($x \approx 0.36$), $^{120}_{48}$Cd ($x \approx 0.39$) and $^{230}_{90}$Th ($x \approx 0.72$) for the non-rotating case ($L = 0$). One, indeed, observes a slight distortion of the energy landscape that is more pronounced for the light nucleus $^{46}_{22}$Ti, but the left–right symmetric shape stays the energetically favoured one.

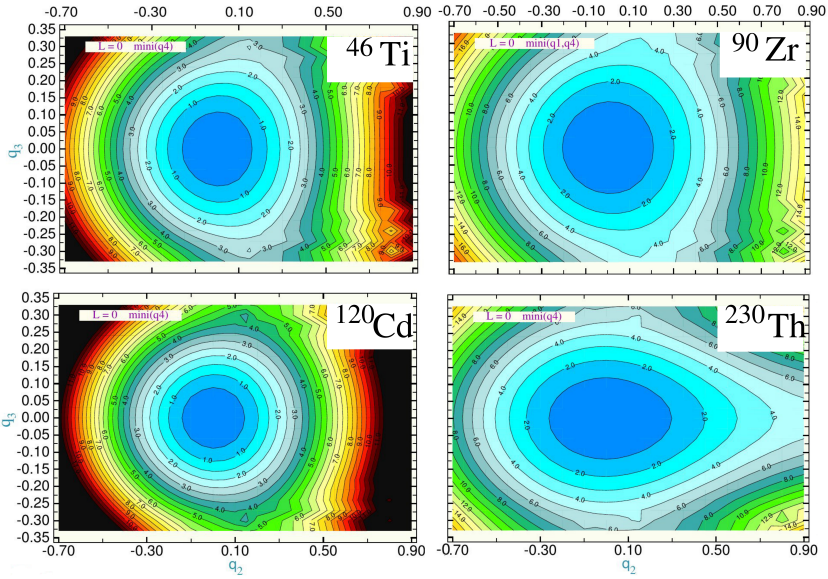

Fig. 1. Nuclear deformation energies for four nuclei from different regions of the periodic table as a function of the elongation parameter q_2 and the left–right asymmetry parameter q_3. Throughout the landscapes, the energy has been minimized with respect to the *hexadecapole* parameter q_4, but the regions of the stationary points are always found to have $q_4 = 0$.

Let us now investigate how this landscape, in particular for that light nucleus, evolved with increasing value of the rotational angular momentum. We thus show in Fig. 2 the same kind of deformation energy as in Fig. 1, as a function of q_2 and q_3, only for $^{46}_{22}$Ti, but for 4 different values of L, namely for $L = 0$, 20, 35 and 40 $\hbar$. These energies have been minimized with respect to the two other deformation parameters, q_4 and η. Please note that for $L = 20\,\hbar$, there are two minima of equal depth appearing. Both of these minima, one on the oblate side with $q_2 < 0$ and $\eta = 0$, one on the prolate side ($q_2 > 0$) with finite η, correspond, in fact, to exactly the same oblate shape because such a shape can be obtained by either considering the z- or say, the x-axis as symmetry axis. In the first case, with rotation around the z-axis, the half axis a and b are equal and larger than the elongation parameter z_0 and, consequently, one has an axially symmetric shape with $\eta = 0$. In the other case, with rotation around the x-axis, one would have $b = z_0 > a$ and, consequently, $\eta > 0$. This simply means that one needs to use some caution when analysing these landscapes, making sure not to introduce some *double counting* of shapes.

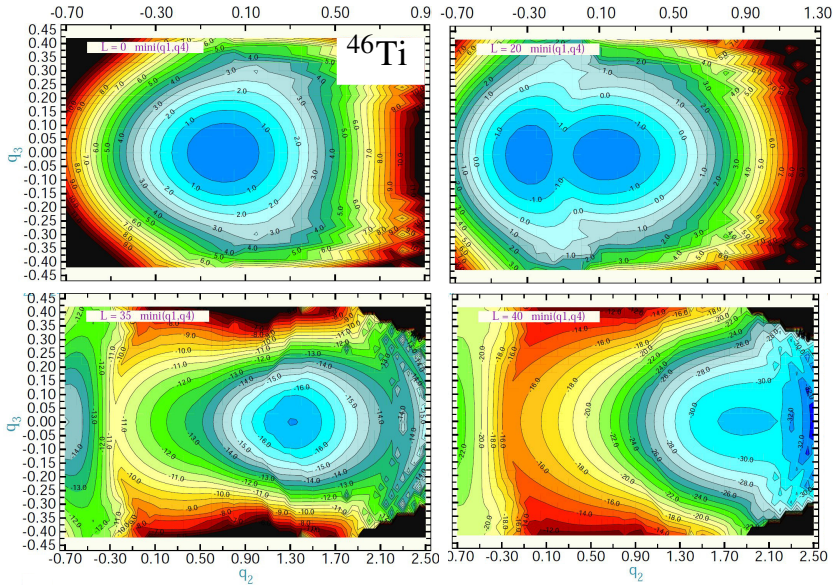

Fig. 2. Deformation energy, as in Fig. 1, for the nucleus $^{46}_{22}$Ti for different values of the angular momentum as indicated inside the figures.

For an angular momentum of $L = 35\,\hbar$, the nucleus has already left the oblate side (Maclaurin regime) and become triaxial (the minimum energy is now obtained at a value of $q_2 > 0$ with a non-axiality parameter $\eta > 0$). At

a still larger values $L = 40\,\hbar$, the stationary point is obtained at very large q_2 with η approaching again zero value. One has now arrived close to the prolate side and close to the scission instability.

Figure 3 shows the same kind of analysis for $^{120}_{48}$Cd. The conclusions are the same as for $^{46}_{22}$Ti. The nucleus stays in the Maclaurin regime of more and more pronounced oblate deformation, as L increases, up to somewhere between 60 and 70 $\hbar$ of angular momentum where the Jacobi instability into triaxial shapes sets in. For the still heavier nuclear system $^{194}_{78}$Pt, one observes again the same picture, except that for an angular momentum of $L \approx 75\,\hbar$, the centrifugal scission point is already reached. In none of these cases, neither at low, nor at high angular momentum, a Poincaré instability into octupole deformed shapes is observed.

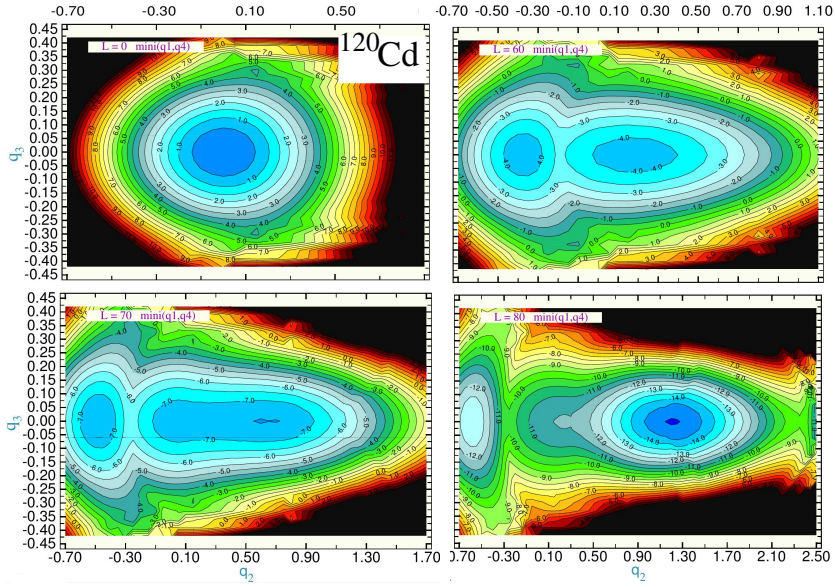

Fig. 3. Deformation energy, as in Fig. 2, for the nucleus $^{120}_{48}$Cd for different values of the angular momentum as indicated inside the figures.

Let us now look more specifically at the Jacobi transition into triaxial shapes. Many years ago, we have already investigated this transition for the nucleus ^{90}Zr [14] in the framework of the selfconsistent semiclassical approach, known as the Extended Thomas–Fermi (ETF) method [15] generalized to rotating nuclei in Ref. [16]. The result of that investigation performed at that time for the Skyrme SkM* interaction [17] is schematically shown, as traditionally done, in the $\beta\gamma$ plane in Fig. 4.

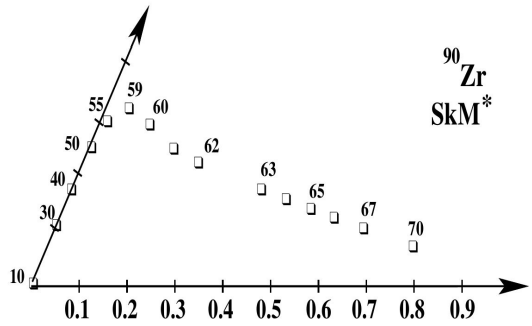

Fig. 4. Deformation of the ETF energy, given in the $\beta\gamma$ plane, for the nucleus ^{90}Zr as a function of the angular momentum.

We would like now to investigate the same nuclear system to check the ability of our new shape parametrization to describe such a transition. The result of this study is shown in Fig. 5. As one can see from the different deformation energy landscapes, one observes the Jacobi transition into triaxial shapes to occur at an angular momentum of $L \approx 55\,\hbar$ and the disruption of the nucleus due to the centrifugal force beyond $L \approx 70\,\hbar$ which is in perfect agreement with the results obtained earlier in the ETF framework.

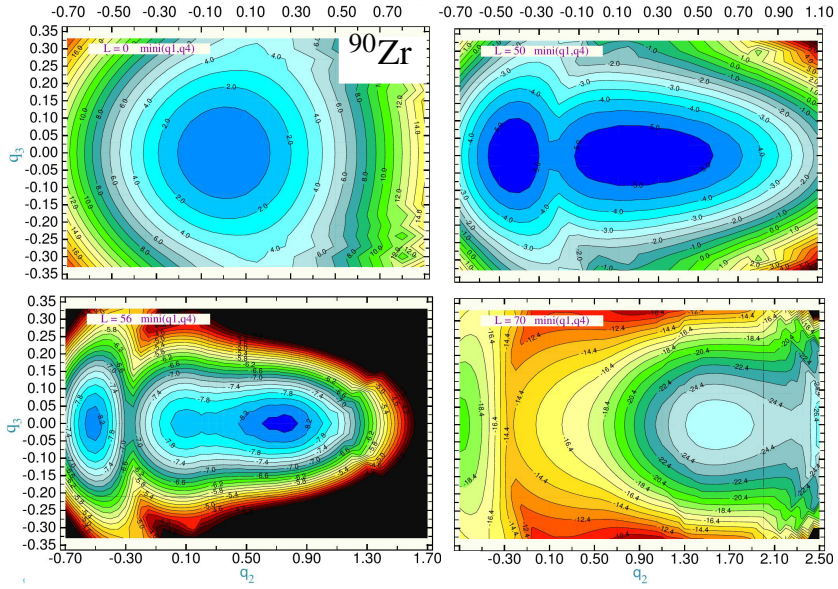

Fig. 5. Deformation energy, as in Fig. 3, for the nucleus ^{90}Zr for different values of the angular momentum as indicated inside the figures.

One would finally like to check the convergence of the Fourier parametrization with respect to higher order terms. We have thus investigated the liquid-drop ground state energies obtained at different L values with respect to the potential impact of higher multipolarity terms and performed that study for several nuclear systems, but show the results, as an example, just for the previously studied ^{90}Zr nucleus. When plotting the energy as a function of the higher-order deformation parameters q_5 and q_6, one notices, however, as seen in Fig. 6, that the minimal energy is always obtained at a zero value of these higher order parameters, thus ensuring the very rapid convergence of the Fourier expansion (2.2), when expressed in the q_n coordinates, even for very large deformations.

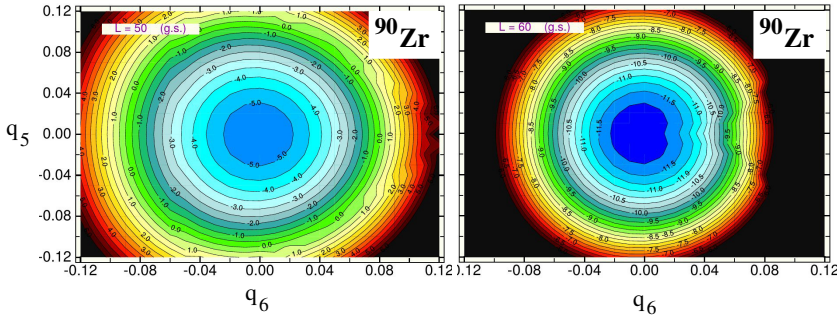

Fig. 6. The liquid-drop type nuclear energy as a function of the higher-order deformation parameters q_5 and q_6 for different values of the angular momentum L. The lower-order Fourier parameters q_1 to q_4 are those of the ground state at these L values.

4. Summary

We have shown that our new Fourier shape parametrizations is very rapidly converging when expressed in the q_n deformation parameters and perfectly able to describe the behaviour of rotating nuclei, in particular, what the different regimes, namely of Maclaurin type and the Jacobi bifurcation into triaxial shapes is concerned. We have also evidenced a distortion of the energy landscape in the direction of left–right asymmetric shapes, in particular, for light nuclei, but no Poincaré instability has been observed. One rather observes that rotation stabilizes the nuclear system against such left–right asymmetric distortions. This conclusion might, of course, change for certain nuclear systems when shell effects are taken into account.

REFERENCES

[1] S. Cohen, F. Plasil, W.J. Swiatecki, *Ann. Phys. (N.Y.)* **82**, 557 (1974).

[2] S. Chandrasekar, *Phys. Rev. Lett.* **24**, 611 (1970).

[3] E. Lottner, C.W. Bockhardt, A. Clebsch, *C.G.J. Jacobi's Vorlesungen über Dynamik*, printed by G. Reimer, Berlin 1884.

[4] H. Poincaré, *Acta Math.* **7**, 259 (1885).

[5] K. Pomorski, J. Dudek, *Phys. Rev. C* **67**, 044316 (2003).

[6] P. Moeller, J.R. Nix, W.D. Myers, W.J. Swiatecki, *At. Data Nucl. Data Tables* **59**, 185 (1995).

[7] B. Nerlo-Pomorska, K. Pomorski, J. Bartel, C. Schmitt, *Acta Phys. Pol. B Proc. Suppl.* **10**, 173 (2017), this issue.

[8] C. Schmitt, K. Pomorski, B. Nerlo-Pomorska, J. Bartel, submitted to *Phys. Rev. C*.

[9] J. Piperova *et al.*, *Nucl. Phys. A* **652**, 142 (1999).

[10] J. Bartel, B. Nerlo-Pomorska, K. Pomorski, *Int. J. Mod. Phys. E* **18**, 986 (2009).

[11] R.W. Hasse, W.D. Myers, *Geometrical Relationships of Nuclear Physics*, Springer Verlag, Heidelberg 1988.

[12] K. Pomorski, J. Bartel, *Int. J. Mod. Phys. E* **15**, 417 (2006).

[13] K. Pomorski, B. Nerlo-Pomorska, J. Bartel, C. Schmitt, *Acta Phys. Pol. B Proc. Suppl.* **8**, 667 (2015).

[14] E. Chabanat *et al.*, *Phys. Lett. B* **325**, 13 (1994).

[15] M. Brack, C. Guet, H.-B. Håkansson, *Phys. Rep.* **123**, 275 (1985).

[16] K. Bencheikh, P. Quentin, J. Bartel, *Nucl. Phys. A* **571**, 518 (1994).

[17] J. Bartel *et al.*, *Nucl. Phys. A* **386**, 79 (1984).